Final Report on DOE Grant No. DE-FG02-03ER46059 Titled: "Structural Transformations in Ceramics: Perovskite-like Oxides and Group III, IV, and V Nitrides"

Period of Proposal: 1 July, 2003–31 Dec, 2006; Excess budgetary funds: None
James P. Lewis (PI, former Co-PI), Dorian M. Hatch (Co-PI, former PI), and Harold T. Stokes (Co-PI)
Department of Physics, West Virginia University, Morgantown, West Virginia 26506
Department of Physics and Astronomy, Brigham Young University, Provo, Utah 84602

1 Overview of Results and their Significance

Ceramic perovskite-like oxides with the general formula $(A'A'' \ldots)(B'B'' \ldots)O_3$and titanium-based oxides are of great technological interest because of their large piezoelectric and dielectric response characteristics.[1] In doped and nanoengineered forms, titantium dioxide finds increasing application as an organic and hydrolytic photocatalyst. The binary main-group-metal nitride compounds have undergone recent advancements of *in-situ* heating technology in diamond anvil cells leading to a burst of experimental and theoretical interest. In our DOE proposal, we discussed our unique theoretical approach which applies *ab initio* electronic calculations in conjunction with systematic group-theoretical analysis of lattice distortions to study two representative phase transitions in ceramic materials: (1) displacive phase transitions in primarily titanium-based perovskite-like oxide ceramics, and (2) reconstructive phase transitions in main-group nitride ceramics. A sub area which we have explored in depth is doped titanium dioxide electrical/optical properties.

Work in displacive phase transitions in ceramic-like perovskite alloys has produced six papers in print (or press)[2, 3, 4, 5, 6, 7], one submitted paper[8], and two in preparation[9, 10], which can be grouped into seven main areas:

(1) We have used domain average engineering symmetry methods to study heterogeneous domain structures in perovskite ferroelectrics. The domain average symmetry that we consider is applicable to crystals having a large number of domains. For such a case, the domains form a kind of nano-composite. The result[2] was a systematic derivation of all allowed "domain sets", their mesoscopic symmetry, information about the role of domain fractions in determining that symmetry, and the corresponding physical tensor properties for that domain set. The three cases we considered in depth corresponded to polarization (p_x, p_y, p_z) oriented along [100], [110], and [111], resulting in the single domain state symmetries $P4mm$, $Amm2$, and $R3m$, respectively. For the [111] polarization direction the PZM-PT and PMN-PT crystals are examples of interest. The well known $BaTiO_3$ is an example of a structural change with polarization along the [100] direction. $KNbO_3$ is an example of a material which undergoes a transition due to the spontaneous polarization toward the edge diagonals $\langle 110 \rangle$. As an example of the results we obtained, the dipole ordering along [100], corresponding to $BaTiO_3$, is shown in Table 1. ISOTROPY contains the computer implementation of our algorithm **for any space group to sub-group phase transition** and is freely available[11].

(2) To validate these theoretical multidomain structures we have developed a fast thermodynamic approach to recreate mesoscopic multidomain ferroelectrics.[3] Using a phase field theory free energy functional we have developed a novel multi-order parameter evolution strategy for ferroelectrics is much faster than previous simulations employing instantaneous mechanical equilibrium[12, 13, 14, 15, 16, 17, 18, 19]. We determined potential coefficients were determined via the techniques of global phase diagrams (GPDs) and have been discussed in detail for molecular crystals[20, 21, 22].

As an example of this work we briefly discuss a [100]-ordering $P4mm$ nanocomposite. As shown in Fig. 1, the symmetry is broken by a Γ_4^- space group irreducible representation with six possible energetically equivalent domains (each a different color). These domains correspond to the multidomain structures given in Table 1. Figure 1 shows that without any reference to the theoretical derivations of Ref. [23], mesoscopic simulations using combinations of external fields have reproduced predicted symmetries. The group theoretical enumeration of all possible multidomain structures and its numerical validation are needed for high precision domain engineering and are vital to a "bottom-up" micro- and nanotechnology materials design approach to achieve macroscopic materials with precise properties.

(3) We are extending this mesoscopic approach to ferroelastics and multiscale first-principles-based simulation of domain structures. Currently the mesocopic structure code (called DOMAINS) determining the dynamics of the free energy uses finite differences and fixed geometries. A better option is to use adaptive finite elements (AFE) and moving geometries. AFE allows the material to change atomic spacings during and after field changes which (a) gives better hysteresis effects, (b) is physically realistic, and (c) is computationally efficient because it uses fewer nodes in the middle of domains. Another improvement is to base our calculations on first principles simulations rather than empirical coefficients. As the QC multiscale method[24] already has many of these features built-in, we are working with its authors to apply it to multidomain structures and extend its *ab initio* capabilities to other materials besides metals.[25] A simple test case for this without the complexity of electric fields would be to model ferroelastic transitions[9]. This was an intended extension of DOMAINS. Other possible extensions in the future include modeling ferroelectric nanodomains useful in quantum dot FeRAMs or phase change memory.

Table 1: Ref. [23] shows there are 12 possible multidomain structures for symmetrically distinct connected sets for ferroelectric ordering along [100]. This corresponds to the $221(Pm\bar{3}m) \rightarrow 99(P4mm)$ transition of $BaTiO_3$. Here we have selected 5 of the 12 possible structures. The "Domain Set" column shows constants such as *a*, *b*, and *c* which represent volume fractions of each domain. The "Group" column gives the point group of the multidomain structure after the convention of Ref. [23]. Columns 3, 4, and 5 give the space group irreducible representations of the external fields and their directions that lead to the domain average engineered structure. Only nonzero contributions of the order parameters are shown in columns 3, 4, 5.

Set	Group	Γ_4^-	Γ_3^+	Γ_5^+
(1,2,3,4,5,6)	$m\bar{3}m$			
(1,2,5,6)	$4_z/m_x m_{xy} m_z$		$(a,0)$	
(3,4)	$4_z/m_x m_{xy} m_z$		$(a,0)$	
(1,3,5)	$3_{xyz} m_{\bar{x}y}$	(a,a,a)		(a,a,a)
(3)	$4_z m_x m_{xy}$	$(0,0,a)$	$(a,0)$	
(3,6)	$m_{yz} m_x 2_{\bar{y}z}$	$(0,a,-a)$	$(a,\sqrt{3}a)$	$(0,a,0)$

(4) We have proposed to use electronic structure methods to obtain bulk properties in PZT materials as well as the free energies associated with phase transformations in such materials. Before considering these more complex PZT ($Pb(Zr_xTi_{1-x})O_3$) systems, we previously investigated properties of simpler TiO_2 systems (also PbS) to validate and benchmark our algorithms and electronic structure methods. This has led to many interesting conclusions and a summary of previous results on bulk and carbon-doped TiO_2[7, 5] are presented here along with new results on other anion-doped forms of TiO_2[6] and TiO_2 internal[8] and surface structure[10]. We also published how ab initio studies can be combined with our mesoscopic symmetry calculations[4].

Previously we outlined our results of the structural, electronic, and elastic properties in both rutile and anatase using the FIREBALL [26] electronic-structure code, which correctly predicts[7] the volume, lattice constants, and atomic positions of rutile and anatase TiO_2 within 0.6% of experimental values[27] and the bulk modulus within 2.4% of experiment[28]. Among other results it gave a direct band gap of 3.05 eV and 3.26 eV (absorbs in UV) at the gamma point for rutile and anatase polymorphs respectively.[5] These predictions are in excellent agreement with the experimental gaps 3.06 eV**[29]** and 3.20 eV**.**[30]

(5) We have recently extended these calculations to anion-doped versions of TiO_2 and their electro-optical properties. It is of great interest to find ways to engineer the absorption wavelength range of TiO_2 into the visible region without a decrease in photocatalytic activity. Impurity doping is frequently used to improve optical absorption.

In carbon doped TiO_2 we found bandgap narrowing due to new half-filled carbon 2p states above the valence band edge at 5.2% C concentration.[5] Other studies confirmed a red shift in the absorption spectra at this concentration.[31, 32, 33, 34, 35, 36] At 0.26% C doped rutile the band is shifted by about the same amount but little overlap with oxygen valence band states occurs. A calculation of the number of accessible atoms per electronic state at 0.26% C doping reveals the valence band edge states are also quite localized. As a result hole mobility is limited, leading to reduced photocatalytic activity. For 5.2% C-doped TiO_2 the states near the valence band edge are delocalized and C states overlap significantly with oxygen atom states. This explains why **higher carbon concentration produces visible absorption with larger photocatalytic efficiency overall**.

In addition to carbon-doped TiO_2 we have also studied nitrogen, phosphorous, and sulfur doping[6]. As N doped TiO_2 augers perhaps the best photocatalytic behavior, we explore this case as an example. Experimental results for doping with nitrogen indicate there is a significant red shift in the absorption spectra which yields photoactivity in the visible.[31] To explore the effects of nitrogen doping a 384 atom supercell of 5.2% and 0.52% substitutional N doped rutile was used to calculate the electronic density of states (DOS) shown in Fig. 2 (a). It is apparent there is no valence band shift for higher N concentrations but a significant shift at lower N concentrations with a bandgap of 2.55 eV, in agreement with experimental observations.[31]

To calculate the degree of electron localization near the band edge a parameter W, which gives the number of accessible atoms in a particular electronic state, is used. Figure 2 (b) shows a scatterplot of W for each electronic state near the valence band edge for 5.20% and 0.52% N doped TiO_2. It has been proposed that the states in the gap should overlap sufficiently with the O_{2p} states to transfer photoexcited carriers to reactive sites at the catalyst surface within their lifetime.[31] The projected DOS onto nitrogen and oxygen atoms (Fig. 2 (a), left) shows there is significant overlap between the nitrogen states and O_{2p} states for 5.20% N doped TiO_2. Figure 2 (b), shows these states are highly delocalized, allowing electrons to reach the surface more easily. On the other hand at lower concentrations the states introduced by N dopants are distinct and highly localized on a single N atom. There is no significant overlap observed for the structures of 0.26% N concentration. And the energy shift of the valence band edge is much smaller compared with the high doping concentration structures. This allows one to **predict that photocatalytic performance for smaller N concentrations should be much lower than that of higher concentrations**.

Figure 1: Distinct [100] ordering multidomain structures after electric field / stress domain average engineering. The original equi-domain structure is on the far left. New multidomain structures after application of external fields labeled by space group irreducible representation (IR) and order parameter direction are on the right. An external electric field has the symmetry of the Γ_4^- IR while compressive and shear stresses have the Γ_3^+ and Γ_5^+ space group symmetries. In a bar plot near each structure is shown the volume fractions of each of the six domains, numbered from the top. Each domain volume fraction is labeled by that predicted by multidomain group theory[23].

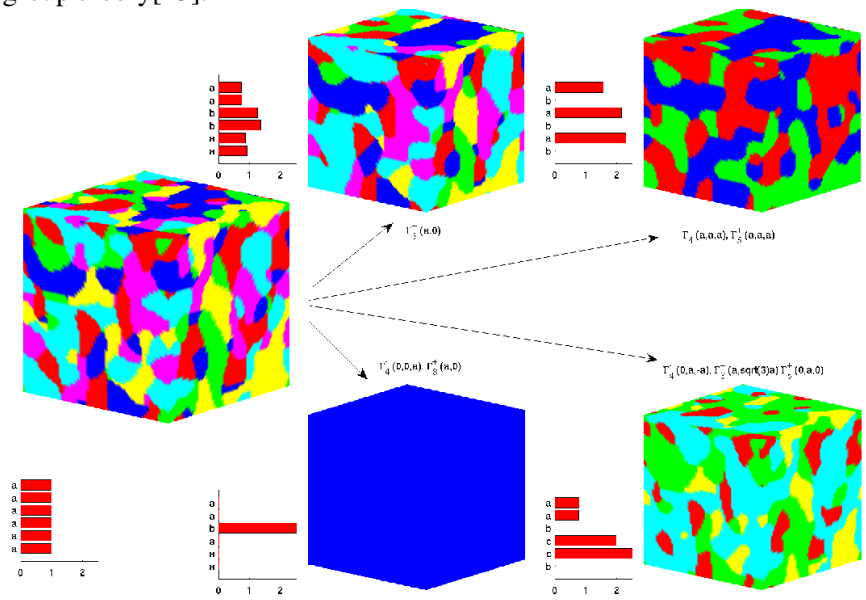

(6) In the original proposal we discussed implementation of a slow growth MD algorithm in FIREBALL to find *ab initio* free energy differences between ceramics with different compositions. We have looked at an initial case of vacancy formation in TiO_2 and have submitted a paper on our results.[8] In transition metal oxides such as TiO_2, bulk and surface oxygen vacancies often dominate the electronic and chemical surface properties[37]. Because of FIREBALL's unique approach to electronic structure, we are able to look at realistic vacancy concentrations (large unit cells) and longer time scales in our slow growth MD runs than typical electronic structure codes.

To find vacancy formation free energies we use nonequilibrium thermodynamic integration[38] (TI) and reversible scaling[39] to find the ab initio free energy difference between a perfect crystal and one with a vacancy as a function of temperature (0-500). This procedure has been implemented into FIREBALL using a novel client/server socket algorithm. Using a 162-atom (much larger than than previous plane wave and Perrot functional calculations using 64- and 54-atom supercells) we find a nonlinear decrease in the reversible work of vacancy formation free energy of 4.5 eV (from 10.8 eV to 6.3 eV) which is driven by entropic effects. Such simulations are useful to control vacancy formation and migration in a well-understood, precisely-controlled way.

With an ab initio thermodynamic integration algorithm in place, we are prepared to examine more complex ceramics which were the subject of this proposal. Many of the technologically important properties of PZN-PT, for example, appear in solid solutions near the morphotropic phase boundary, making the study of free energy differences between the phases essential. Although we have not currently performed PZN-PT compositional simulations by changing Zn/Nb to Ti, all the computational tools to do so are in place. Thus our future plans include microscopic modeling of free energy changes between these materials and between differing space group structures such as the rhombohedral to tetragonal structure in PZN-PT. A possible further extension then is to combine this with QC-type multiscale modeling to optimize piezoelectric functionality (i.e. transducer/actuator/biosensor design).

7) In addition to bulk, doped, vacancy, and multidomain structures of titanium based or perovskite-like oxides, we are also studying TiO_2 surface phases based on oxygen coverage. To better understand the technologically important area of surface vacancies which are directly involved in surface catalysis, we have completed a systematic study of the correlation between defect concentration and surface energy. We have found that the surface energy of TiO_2 decreases from 0.0% to 50.0% coverage, stays low from 50.0% to 75.0% coverage, and increases from 75.0% to 100.0% coverage[10], which agrees with oxygen adsorption studies[40, 41]. In conjunction with this calculation we are preparing oxygen adatom simulations using thermodynamic integration which will give the free energetic barrier of O_2 adsorption as a function of temperature.

Progress in the area of energetically favorable pathways in reconstructive transitions has produced four published papers[42, 43, 44, 45] and one paper submitted[46]. They all obtain a listing of transition pathways (using COMSUBS) and then determine

Figure 2: (a): Electronic density of states (DOS) for N doped rutile TiO_2 at 5.2% (left) and 0.52% (right) concentrations. The dashed line indicates the valence band edge in the system. The top panel shows the DOS for bulk TiO_2 as a reference, the second panel shows the N doped structure, and the third and lowest panels show the projected DOS onto nitrogen and oxygen atoms, respectively. (b): Accessible atoms per electronic state for N doped TiO_2. 5.2% and .52% doping concentrations are shown on the left and right. The dashed line is the valence band edge.

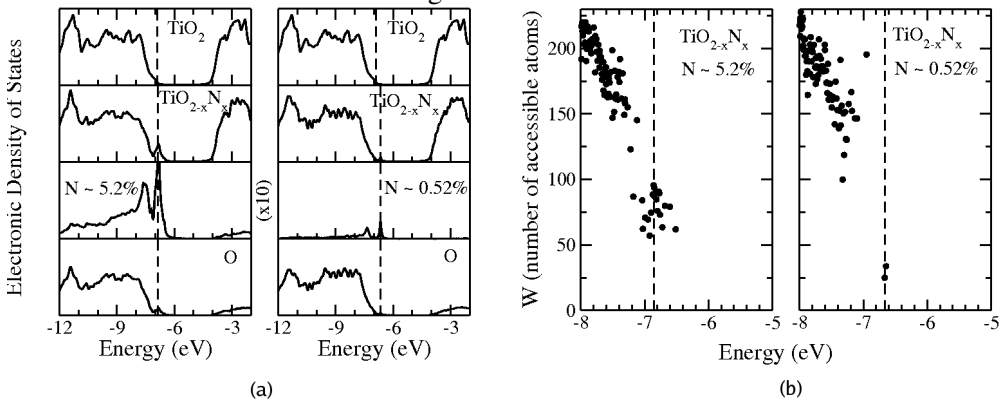

Figure 3: (a) Reversible work of vacancy formation as a function of temperature. For comparison, the dashed line shows a linear trend. (b) (111) planes of atoms in the ZB and RS structures. The open circles represent Si atoms, and the filled circles represent C atoms. In the transition from ZB to RS, the top two planes slide with respect to the bottom plane.

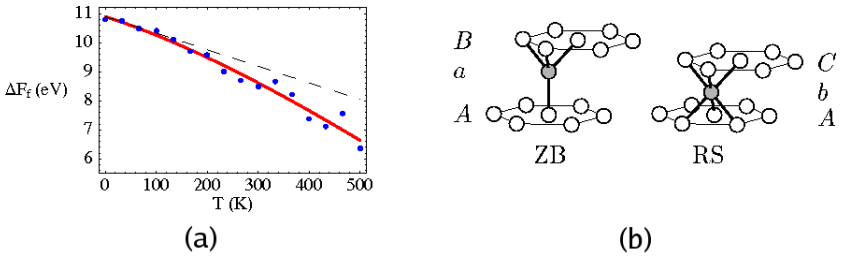

the most favorable pathway using electronic structure methods. COMSUBS has undergone various improvements during the funding of this grant, many of which are reviewed in the previous progress report. They have contintued to make COMSUBS more efficient so that it can handle a large number of atomic mappings.

Papers in the area of reconstructive transitions analyze the $B1$ to $B2$ types of transitions in NaCl and PbS[42], the zinc-blend to rocksalt transition in SiC[45], the α to ω transition in titanium[44], and the wurtzite to rocksalt transition in GaN[46]. As an example let us examine the bilayer sliding mechanism for the zinc-blende to rocksalt transition in SiC.

We used COMSUBS to find possible transition paths (TPs) from the zincblende to the rocksalt structure and obtained 925 possible TPs. For each of these TPs, we used FIREBALL to estimate the enthalpy barrier by varying lattice parameters and atomic positions linearly between the ZB to the RS structures. This obviously overestimates the true barrier height but provides an efficient way to determine which of the 925 TPs should be further considered as likely mechanisms for the phase transition.

This screening resulted in eight TPs that were clearly much lower in enthalpy than the 925 TPs found by COMSUBS. Previous theoretical studies of structural phase transitions have primarily considered only high-symmetry TPs with a small number of structural parameters. In contrast, our current study includes low-symmetry TPs with a large number of structural parameters and therefore imposes computational challenges for finding how the structural parameters vary along the true TP.

We have developed an efficient numerical algorithm (called the bow-function method) for finding the true saddle point along each TP and which is described in Ref. [45]. The TPs we obtained helped us discover a bilayer sliding mechanism common to all eight TPs with the lowest barriers (see Fig 3(b) for an illustration). Furthermore, it is only with the help of these TPs that we could have discovered how the barrier height is lowered by allowing different bilayers to slide at different rates. When a large number of structural parameters are present, the bow-function method is a powerful tool for investigating TPs in reconstructive phase transitions.

2 Personnel

This research is being conducted through the PI James P. Lewis, and the two Co-PI's Dorian M. Hatch and Harold T. Stokes. We have one post-doctoral research associate, J. Brandon Keith, working with us since Jan 2005. He has been spending his time working on the simulation of multidomain formation in multiferroic perovskite systems and implementing the slow growth algorithm in FIREBALL. Hao Wang (Visiting Research Professor) is partly supported by this grant; he collaborates with Dr. Stokes on electronic structure calculations of the reconstructive phase transitions and Dr. Lewis on electronic structure calculations in TiO_2 materials. We have had three PhD graduate students (Jesse Gunter, Grigory Roubtsov, and Anton Nikiforov) working with us as well as two undergraduates (Richard Hansen and Jason Ard) during a large portion of this funded research.

3 Current and Pending Support

3.1 Current Support

- "Structural Transformations in Ceramics: Perovskite-like Oxides and Group III, IV, and V Nitrides"; PIs - Dorian Hatch (BYU), James P. Lewis (WVU), Harold Stokes (BYU); DOE Basic Science Program; total funding $283,556 (1 July 2003 - 1 Jan 2007).

- "Theoretical Investigation of the Surface Effects in II-VI and III-V Semiconducting Nanocrystals"; PI - James P. Lewis; NIST Physics Program; total funding $99,890 (1Jul 2004 - 30 Jun 2007).

- "ITR: Development of a Web-Based Grid-Compuiting Environment for Research and Education in Computational Science and Engineering"; PIs - Thanh N. Truong, Thomas E. Cheatham, III, Chuck Wight (UofU), and James P. Lewis (WVU); NSF-ITR Program; total funding $3.2 million, subaward to BYU - $313,261 (1 Sep 2003 - 31 Aug 2007).

- "Collaborative Research: Nanospace Perspective of Bacterium-Mineral Interface"; PIs - Barry Bickmore (BYU), James P. Lewis (WVU), and Steven K. Lower (Ohio State); NSF-Biogeosciences; total funding (BYU) - $355,873 (1 Sep 2005 - 31 Aug 2009).

- "High-Throughput Ab Initio Modeling of Charge and Spin Transport for Bio-Molecular-Electronics and Spintronics"; PIs - Roger Lake (UC-Riverside) and James P. Lewis (WVU); NSF-ECS; total funding $374,908 (1 Sep 2005 - 31 Aug 2008).

3.2 Pending Support

- "Investigation of Charge Transfer and Reaction Mechanisms in Photocatalysis at the Interfaces of Surfaces and TiO_2"; PIs - James P. Lewis (WVU) and Bret Hess (BYU); DOE; (in preparation).

4 Invited and Contributed Presentations

- J. B. Keith, H. Wang, D. M. Hatch, and J. P. Lewis, "Anion doping of TiO_2, free energies of vacancy formation in TiO_2, and ferroelectric domain engineering", *6th Pacific Rim Conference of the American Ceramic Society*, Kapalua, HI, Sept 2005.

- H. T. Stokes, D. M. Hatch, J.-J. Dong, J. Gunter, H. Wang, and J. P. Lewis, "Bilayer Sliding Mechanism for the Zincblende to Rocksalt Transition in SiC", *March Meeting of the American Physical Society*, Los Angeles, 21 Mar 2005.

- H. Wang and J.P. Lewis, "Effects of Dopant States on the Electronic Structures in Tungsten Doped TiO_2*," March Meeting of the American Physical Society*, Los Angeles, 21 Mar 2005.

- J. P. Lewis and H. Wang, "Second Generation Photocatalytic Materials - Anion Doped TiO_2," *March Meeting of the American Physical Society*, Los Angeles, 21 Mar 2005.

- J. Gunter, H. T. Stokes, D. M. Hatch, and J. P. Lewis, "Mechanism of the Wurtzite-to-Rocksalt Phase Transition in GaN", *19th Annual Spring Research Conference*, Brigham Young University, Provo, UT, 19 Mar 2005.

- R. Hansen, H. T. Stokes, D. M. Hatch, and J. P. Lewis, "Computer Analysis of FCC-HCP Structural Phase Transition in Pb", *19th Annual Spring Research Conference*, Brigham Young University, Provo, UT, 19 Mar 2005.

- J.P. Lewis, "Second Generation Photocatalytic Materials - Anion Doped TiO_2," *Seminar*, Computational Materials Science Group, Oak Ridge National Laboratory, 10 Feb 2005.
- J.P. Lewis, "Second Generation Photocatalytic Materials - Anion Doped TiO_2," *Colloquium*, Department of Physics, Utah Valley State College, 8 Dec 2004.
- J.P. Lewis, "Second Generation Photocatalytic Materials - Anion Doped TiO_2," *Seminario*, Facultad de Ciencias, Universidad Autonoma de Madrid, Spain, 26 Oct 2004.
- J. Gunter, J. P. Lewis, H. Stokes, and D. M. Hatch, "Transitions in SiC," *American Physical Society Four Corners Meeting*, Tempe, Arizona, Oct 2003.

5 Publications

- J. B. Keith, J. P. Lewis, and D. M. Hatch. "A multiscale treatment of ferroelastic domain formation," (in preparation).
- Z. G. Wei, J. B. Keith, H. Wang, and J. P. Lewis. "Defect-mediated rutile TiO_2 (110) surface energy and ab initio free energy of O_2 adsorbtion," (in preparation).
- J. B. Keith, H. Wang, and J. P. Lewis. "Free energies of vacancy formation in TiO_2using accelerated ab initio nonequilibrium thermodynamics," (submitted in August, 2006).
- H. T. Stokes, J. Gunter, D. M. Hatch, J.-J. Dong, H. Wang, and J.P. Lewis, "Bilayer sliding mechanism for the wurtzite-to-rocksalt transition in GaN," (submitted).
- J. B. Keith and D. M. Hatch. "Mesoscopic domain average engineering simulations of ferroelectric perovskites compared with multidomain group theoretical predictions," *J. Appl. Phys.* (in press).
- J. B. Keith, D. M. Hatch, H. Wang, and J. P. Lewis. "Application of computational ceramic engineering to titanium dioxide photocatalysis, defect free energies of formation, and domain average engineering of ferroelectrics," *Ceramic Transactions* (in press).
- H. Wang and J. P. Lewis. "Second-generation photocatalytic materials: anion-doped TiO_2," *J. Phys. Condens. Mat.* 18, 421 (2006).
- D. M. Hatch, H. T. Stokes, J. J. Dong, J. Gunter, H. Wang, and J. P. Lewis, "Bilayer sliding mechanism for the zinc-blende to rocksalt transition in SiC", *Phys. Rev. B* 71, 184109 (2005).
- D. R. Trinkle, D. M. Hatch, H. T. Stokes, R. G. Hennig, and R. C. Albers, "Systematic pathway generation and sorting in martensitic transformations: Titanium alpha to omega," *Phys. Rev. B* 72, 014105 (2005).
- H. T. Stokes and D. M. Hatch, "FINDSYM: program for identifying the space-group symmetry of a crystal," *J. Appl. Cryst.* 38, 237 (2005).
- H. Wang and J. P. Lewis. "Effects of dopant states on photoactivity in carbon-doped TiO_2," *J. Phys.: Condens. Mat.* 17, L209 (2005).
- P. Jelinek, H. Wang, J.P. Lewis, O.F. Sankey, and J. Ortega. "A new multi-center approach to the exchange-correlation interactions in ab inito tight-binding methods," *Phys. Rev. B* 71, 235101 (2005).
- H. T. Stokes, D. M. Hatch, J. Dong, and J. P. Lewis, "Mechanisms for the reconstructive phase transition between the B1 and B2 structure types in NaCl and PbS," *Phys. Rev. B* 69, 174111 (2004).
- D. M. Hatch, H. T. Stokes, and W. Cao, "Allowed mesoscopic point group symmetries in domain average engineering of perovskite ferroelectric crystals," *J. Appl. Phys.* 94, 5220-5227 (2003).

References

[1] S. E. Park and T. R. Shrout, Ultrahigh strain and piezoelectric behavior in relaxor based ferroelectric single crystals, J. App. Phys. **82**, 1804 (1997).

[2] D. M. Hatch, H. T. Stokes, and W. Cao, Allowed mesoscopic point group symmetries in domain average engineering of perovskite ferroelectric crystals, J. App. Phys. **94**, 5220 (2003).

[3] J. B. Keith and D. M. Hatch, Mesoscopic domain average engineering simulations of ferroelectric perovskites compared with multidomain group theoretical predictions, in press, 2006.

[4] J. B. Keith, D. M. Hatch, H. Wang, and J. P. Lewis, Application of computational ceramic engineering to titanium dioxide photocatalysis, defect free energies of formation, and domain average engineering of ferroelectrics, in press, 2006.

[5] H. Wang and J. P. Lewis, Effects of dopant states on photoactivity in carbon-doped TiO_2, J. Phys.: Condens. Matter **17**, L209 (2005).

[6] H. Wang and J. P. Lewis, Second-generation photocatalytic materials: anion-doped TiO_2, J. Phys.: Condens. Matter **18**, 421 (2006).

[7] P. Jelinek, H. Wang, J. P. Lewis, O. F. Sankey, and J. Ortega, A new multi-center approach to the exchange-correlation interactions in ab initio tight-binding methods, Phys. Rev. B **71**, 235101 (2005).

[8] J. B. Keith, H. Wang, and J. P. Lewis, Free energies of vacancy formation in TiO_2 using accelerated nonequilibrium thermodynamics, submitted in August, 2006.

[9] J. B. Keith, J. P. Lewis, and D. M. Hatch, A multiscale treatment of ferroelastic domain formation, In preparation, 2006.

[10] Z.-G. Wei, J. B. Keith, H. Wang, and J. P. Lewis, Defect-mediated TiO_2 (110) surface energy and ab initio free energy of O_2 adsorbtion, In preparation, 2006.

[11] H. T. Stokes and D. M. Hatch, Isotropy Software Package, http://stokes.byu.edu/isotropy.html, 2004.

[12] R. Ahluwalia and W. Cao, Influence of dipolar defects on switching behavior in ferroelectrics, Phys. Rev. B **63**, 012103 (2000).

[13] R. Ahluwalia and W. Cao, Size dependence of domain patterns in a constrained ferroelectric system, J. App. Phys. **89**, 8105 (2001).

[14] R. Ahluwalia and W. Cao, Effect of surface induced nucleation of ferroelastic domains on polarization switching in constrained ferroelectrics, J. App. Phys. **93**, 537 (2001).

[15] R. Ahluwalia, T. Lookman, A. Saxena, and W. Cao, Piezoelectric response of engineered domains in ferroelectrics, **84**, 3450 (2004).

[16] S. Nambu and D. A. Sagala, Domain formation and elastic long-range interaction in ferroelectric perovskites, Phys. Rev. B **50**, 5838 (1994).

[17] H. L. Hu and L. Q. Chen, Computer simulation of 90^o ferroelectric domain formation in two-dimensions, Mat. Sci. and Eng. A **238**, 182 (1997).

[18] H. L. Hu and L. Q. Chen, Three-Dimensional Computer Simulation of Ferroelectric Domain Formation, J. Am. Cer. Soc. **81**, 492 (1998).

[19] W. Cao, S. Tavener, and S. Xie, Simulation of boundary condition influence in a second-order phase transition, J. App. Phys. **86**, 5739 (1999).

[20] J. A. Mettes, J. B. Keith, and R. B. McClurg, Molecular crystal global phase diagrams. 1. Method of construction, Acta Cryst. A **60**, 621 (2004).

[21] J. B. Keith, J. A. Mettes, and R. B. McClurg, Molecular crystal global phase diagrams., Crystal Growth and Design **4**, 1009 (2004).

[22] J. B. Keith and R. B. McClurg, Molecular Crystal Global Phase Diagrams II: Reverse Engineering the Intermolecular Potential, In preparation, 2005.

[23] D. M. Hatch, H. T. Stokes, and W. Cao, Allowed mesoscopic point group symmetries in domain average engineering of perovskite ferroelectric crystals, J. App. Phys. **94**, 5220 (2003).

[24] www.qcmethod.com.

[25] G. Lu, E. B. Tadmor, and E. Kaxiras, From electrons to finite elements: A concurrent multiscale approach for metals, Phys. Rev. B **73**, 024108 (2006).

[26] J. P. Lewis, K. R. Glaesemann, G. A. Voth, J. Fritsch, A. A. Demkov, J. Ortega, and O. F. Sankey, Further developments in the local-orbital density-functional theory tight-binding method: FIREBALL, Phys. Rev. B **64**, 195103 (2001).

[27] J. K. Burdett, T. Hughbanks, G. J. Miller, J. J. W. Richardson, and J. V. Smith, Structural-electronic relationships in inorganic solids: Powder neutron diffraction studies of the rutile and anatase polymorphs of titanium dioxide at 15 and 295 K, J. Am. Chem. Soc. **109**, 3639 (1987).

[28] T. Arlt, M. Bermejo, M. A. Blanco, L. Gerward, J. Z. Jiang, J. S. Olsen, and J. M. Recio, High-pressure polymorphs of anatase TiO_2, Phys. Rev. B **61**, 14414 (2000).

[29] J. Pascual, J. Camassel, and H. Mathieu, Fine structure in the intrinsic absorption edge of TiO_2, Phys. Rev. B **18**, 5606 (1978).

[30] R. Sanjinès, H. Tang, H. Berger, F. Gozzo, G. Margaritondo, and F. Lèvy, Electronic structure of anatase, J. App. Phys. **75**, 2945 (1994).

[31] R. Asahi, T. Morikawa, T. Ohwaki, K. Aoki, and Y. Taga, Visible-light photocatalysis in nitrogen-doped titanium oxides, Science **293**, 269 (2001).

[32] S. Sakthivel and H. Kisch, Daylight photocatalysis by carbon-modified titanium dioxide, Angew. Chem. Int. Ed. **42**, 4908 (2003).

[33] H. Irie, Y. Watanabe, and K. Hashimoto, Carbon-doped anatase TiO_2 powders as a visible-light sensitive and photocatalyst, Chem. Lett. **32**, 772 (2003).

[34] S. U. M. Khan, M. Al-Shahry, and J. W. B. Ingler, Efficient photochemical water splitting by a chemically modified n-TiO_2, Science **297**, 2243 (2002).

[35] K. Noworyta and J. Augustynski, Spectral photoresponses of carbon-doped TiO_2 film electrodes, Electrochem. Sol.-St. Lett. **7**, E31 (2004).

[36] L. Zhang and R. V. Koka, A study on the oxidation and carbon diffusion of TiC in alumina-titanium carbide ceramics using XPS and Raman spectroscopy, Mater. Chem. Phys. **57**, 23 (1998).

[37] R. Schaub, E. Wahlstrom, A. Ronnau, E. Laegsgaard, I. Stensgaard, and F. Besenbacher, Oxygen-mediated diffusion of oxygen vacancies on the TiO_2(110) surface, Science **299**, 377 (2003).

[38] M. de Koning, S. R. de Debiaggi, and A. M. Monti, Atomistic calculation of vacancy-formation free energies by reversible vacancy creation, Phys. Rev. B **70**, 054105 (2004).

[39] M. de Koning, A. Antonelli, and S. Yip, Phys. Rev. Lett. **83**, 3973 (1999).

[40] W. S. Epling, C. H. F. Peden, M. A. Henderson, and U. Diebold, Evidence for oxygen adatoms on TiO_2(110) resulting from O_2 dissociation at vacancy sites, Surf. Sci. **412**, 333 (1998).

[41] M. A. Henderson, W. S. Epling, C. L. Perkins, C. H. F. Peden, and U. Diebold, Interaction of molecular oxygen with the vacuum-annealed TiO_2(110) Surface: Molecular and Dissociative Channels, **103**, 5328 (1999).

[42] J. D. H. T. Stokes, D. M. Hatch and J. P. Lewis, Mechanisms for the reconstructive phase transition between the B1 and B2 structure types in NaCl and PbS, Phys. Rev. B **69**, 174111 (2004).

[43] H. Stokes and D. Hatch, FINDSYM: program for identifying the space-group symmetry of a crystal, J. Appl. Cryst. **38**, 237 (2005).

[44] D. R. Trinkle, D. M. Hatch, H. T. Stokes, R. G. Hennig, and R. C. Albers, Systematic pathway generation and sorting in martensitic transformations: Titanium alpha to omega, Phys. Rev. B **72**, 014105 (2005).

[45] D. M. Hatch, H. T. Stokes, J. J. Dong, J. Gunter, H. Wang, and J. P. Lewis, Bilayer sliding mechanism for the zinc-blende to rocksalt transition in SiC, Phys. Rev. B **71**, 184109 (2005).

[46] H. T. Stokes, J. Gunter, D. M. Hatch, J.-J. Dong, H. Wang, and J. Lewis, Bilayer sliding mechanism for the wurtzite-to-rocksalt transition in GaN, In preparation.